

# Metal Streak Analysis with different Acquisition Settings in Postoperative Spine Imaging: A Phantom Study

N.D. Osman, M.S. Salikin, M.I. Sariipan

**Abstract**—CT assessment of postoperative spine is challenging in the presence of metal streak artifacts that could deteriorate the quality of CT images. In this paper, we studied the influence of different acquisition parameters on the magnitude of metal streaking. A water-bath phantom was constructed with metal insertion similar with postoperative spine assessment. The phantom was scanned with different acquisition settings and acquired data were reconstructed using various reconstruction settings. Standardized ROIs were defined within streaking region for image analysis. The result shows increased kVp and mAs enhanced SNR values by reducing image noise. Sharper kernel enhanced image quality compared to smooth kernel, but produced more noise in the images with higher CT fluctuation. The noise between both kernels were significantly different ( $P < 0.05$ ) with increment of noise in the bone kernel images (mean difference = 54.78). The technical settings should be selected appropriately to attain the acceptable image quality with the best diagnostic value.

**Keywords**—Computed tomography, metal streak, noise, CT fluctuation.

## I. INTRODUCTION

THE assessment of the postoperative spine after implantation of fusion or stabilization metallic devices is performed by a wide range of medical imaging modalities. The computed tomography (CT) is preferable modalities to obtain details imaging of bony part with accurate cross sectional anatomical view. However the CT assessment of postoperative spine may happen to be challenging due to occurrence of the metal-induced artifacts [1,2,3]. The artifacts can severely deteriorate the quality of CT images, resulted in obscure anatomical and pathological evaluation and mislead the diagnosis interpretation.

The metal streaking artifacts in CT image are caused by attenuation of high dense metallic implant that lead to missing projection data and beam hardening [4,5].

N.D. Osman is with the Faculty of Health Science, Mara University of Technology Malaysia, 42300 Bandar Puncak Alam, Selangor, Malaysia (phone: +603-32584300; e-mail: diyanaosman.dina@gmail.com).

M.S. Salikin also with the Department of Medical Imaging, Faculty of Health Science, Mara University of Technology Malaysia, 42300 Bandar Puncak Alam, Selangor, Malaysia.(e-mail: saion@salam.uitm.edu.my).

M.I. Sariipan is with the Department of Computer and Communication Systems Engineering, Faculty of Engineering, Universiti Putra Malaysia, 43400 Serdang, Selangor, Malaysia. (e-mail: iqbal@eng.upm.edu.my).

Author would like to acknowledge Advanced Medical and Dental Institute, Universiti Sains Malaysia & Ministry of Higher Education, Malaysia for fellowship sponsorship under Academic Staff Training Scholarship (ASTS/SLAB).

The metallic object absorbed the incident beam causing insufficient photons to be detected (photon starvation), and generate incomplete projection profiles. As the missing data is converted into the reconstructed CT image, they will appear as bright and dark streak due to limited capability of common CT reconstruction algorithm to handle the missing data and inaccurate beam hardening correction [6].

In order to obtain an excellence image quality, knowledge on factors affecting the artifacts and technique to minimize the artifacts is crucially important [5,7]. Previous study have show that the streaking artifacts may be influenced by several technical aspects in the postoperative CT imaging setting such as tube current (in mA), X-ray kilovolt peak (kVp), reconstruction algorithm (kernel), reformatted thickness, hardware composition, geometry (shape), and position [2,5,8,9]. In this article, a phantom study was conducted and the magnitudes of streaks were examined by varying the acquisition and reconstruction parameters via images analysis.

In this paper, analysis is done using both qualitative and quantitative observation. The quantitative part by statistical analysis is important due to limitation in human perception particularly in the ability to integrate the noise in images and conflict exists on individual decision criteria. Therefore, the influences of all the factors on reconstructed images were analyzed statistically by measuring CT attenuation, noise of streaking images.

## II. MATERIALS AND METHODS

### A. Designation and Fabrication of Phantom

A circular water-bath phantom was designed with dimension of 20cm x 15cm x 0.8cm and was made of clear polymethyl methacrylate (PMMA). A hole was drilled at phantom floor for the insertion of Teflon rod which was used to stimulate the composition of boney structures (spine). Two Teflon rods with 50mm diameter and 168mm long were used.

The first Teflon rod accommodates holes for a pair of Titanium and Stainless Steel rods. Both metal types are the common materials used for medical implants. The second Teflon rod hold a pair of spinal screws made up of Titanium that were inserted at 40° from the centre line, similar to the clinical procedure for spinal fusion.

TABLE I  
SCANNING PROTOCOLS FOR PHANTOM STUDY

Parameters	Protocol 1	Protocol 2	Protocol 3	Protocol 4
Scan mode	Abdominal sequential	Abdominal sequential	Abdominal sequential	Abdominal sequential
No. of individual scans	16	16	8	10
Acquisition settings	200 MAS; Different KVP (80, 100, 120, 140 kVP);	120 kVP; Different MAS (100, 200, 300, 400 MAS)	120 kVP; 200 MAS	120 kVP; 200 MAS
Reconstruction kernels	Smooth & sharp kernel	Smooth & sharp kernel	Various kernels (B25s, B31s, B70s, B80s)	Smooth & sharp kernel
Reconstruction thickness	3mm, 6mm	3mm, 6mm	3mm, 6mm	Various thickness (2.4, 3.0, 6.0, 7.2, 9.0mm)

### B. Phantom Study

The phantom was filled with water to create a homogenous surrounding for the ease of attenuation fluctuation and noise measurement. The experimental setup of the phantom scanning is shown in Fig.1. All the phantom scanning was done using a Siemens SOMATOM Definition AS+ Computed Tomography, CT (Siemens Healthcare, Germany) at the Radiology Department in Hospital Universiti Sains Malaysia (HUSM) in Kelantan, Malaysia. The helical CT scanner has 64 rows of detectors, gantry speed of 0.3sec per rotation, and able to produce 128 slices per rotation.

All scans were done in abdominal sequential mode with field of view (FOV) of 230mm. All the phantom images were acquired using four different protocol by varying the acquisition parameters, the tube current and voltage (Table 1). The control images were acquired by scanning the phantom without metal insert followed by phantom scanning with metal insertion in the phantom.



Fig. 1 The setup for phantom scanning in CT scanner

### C. Image Reconstruction

The axial cross-sectional images were reconstructed using the acquired raw data. All images data were reconstructed at standard resolution (512 x 512 pixels). The raw data obtained by the first and second protocol were reconstructed with common reconstruction kernel; B25s and B70s and slice thicknesses of 3.0mm and 6.0mm.

The third raw dataset obtained from third protocol were reconstructed with four different reconstruction kernels (Soft-tissues kernel; B25s-smooth, B31s-medium smooth, and bone kernels; B70s-sharp, B80s-ultra sharp), by reconstructed slice thicknesses of 3.0mm and 6.0mm (Table 1).

Subsequently, raw data obtained with protocol 4 were reconstructed by different reconstruction/slice thickness of 2.4mm, 3.0mm, 6.0mm, 7.2mm, and 9.0mm. For both datasets, the acquisition was constant at 120kVP, and 200MAS.

### D. Metal Streak Analysis

All the phantom images were viewed at CT workstation (CT Syngo Acquisition Workplace, Siemens Medical Solutions, Germany), which equipped with commercial software (Syngo 2010B version). The software is capable of defining region of interest (ROI) and calculating the mean attenuation in Hounsfield unit (HU) and standard deviation (SD) for each ROI.

Analyzed images were all thresholded at the same window width (WW) and level (WL) for visual comparisons; abdomen setting – WW 300, WL 40 and bone setting - WW 1500, WL 450.

Overall, 50 streaking images were analyzed to obtain 1625 attenuation measurements using ROI-based quantitative analysis. Standardized ROI of areas approximately 4mm<sup>2</sup> were drawn on the selected control and various streaking images. The ROIs were set within dark streaking region and bright streaking region around the metal samples.

All attenuation data were displayed as mean HU ± SD. All attenuation data were displayed as mean ± standard deviation which automatically measured using the Syngo CT Software.

Noise,  $\sigma$  in CT images was expressed as the standard deviation within the ROIs. The expression as given by Kalender [10]:

$$\sigma = C_R \sqrt{\frac{I_o / I}{\epsilon QS}} \quad (1)$$

In equation (1), the  $C_R$  is known as the reconstruction algorithm (filter / kernel),  $\epsilon$  is the overall system efficiency,  $Q$  is the product of tube current – scan time (mAs), and  $S$  is the slice thickness. The ratio of  $I_o/I$  refers to attenuation of the object.

The signal-to-noise ratio (SNR) was calculated from the result of HU (signal) and noise obtained through phantom study, as stated by Paul et al [11].

$$SNR = \frac{HU}{Noise, \sigma} \quad (2)$$

For statistical analysis, the mean differences of CT attenuation, noise, and SNR were calculated and compared using statistical T-test performed by SPSS software. If the p-value <0.05, the mean difference is considered as statistically significant.

A correlation analysis was also conducted to study the relationship between the varying acquisition and reconstruction parameters with measured variables such as noise, CT attenuation, and SNR within the streaking region. Correlation is considered significant at p-value <0.05.

### III. RESULTS

Our study shows that metal-induced artifacts appear as bright and dark bands (streaking) in the reconstructed images (Fig. 4). Streaks can be seen in two directions. The dark streaks were more prominent in the direction of the metal screw position (highest attenuation), whereas the bright streaks were more at the transverse direction of the screw.

The appearance of dark streak is due to beam hardening effects which produce high frequency projections, while the low frequency projections due to scattering effects appear as bright streak.

#### A. Different kVp settings

From the qualitative assessment of the images acquired by different kVp setting, it shows that streaking effect reduced with increased kVp. The bright streak area in the images was reduced using high kVp setting.

Measured CT attenuation values were increased (4% - 24%) within dark streak and decreased (15% - 46%) at bright streak region. Image noise is reduced in the images with increased kVp setting with 13 -14% reduction.

From the results, the influence of kVp setting on CT attenuation and image noise was more prominent in bright region compared to dark streak region. The mean difference of CT attenuation and noise are statistically significantly ( $P < 0.001$ ) in bright streak but demonstrated no significant different in dark streak region ( $P > 0.05$ ).

The result also shows significant correlation between the kVp with CT attenuation and image noise ( $P < 0.05$ ) with strong negative correlation in CT attenuation ( $r = 0.98$ ) and noise ( $r = 0.97$ ). The negative correlation means the CT attenuation and image noise decreased as kVp increased.

Higher kVp also resulted in better SNR by increment of 2% in dark streak region and 5% increment in bright region as shown in Fig.2. From data previously published, it is recommended to use 140kVp for imaging of spines with metal hardware [2,8]. Conversely, with higher kVp used, the dose to patient will also increase.

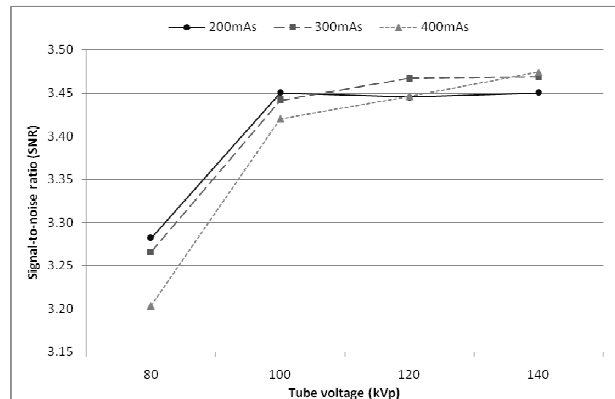


Fig. 2 Graph of signal-to-noise ratio, SNR (y) against reconstruction thickness (x) for different mAs setting in bright streak region.

#### B. Different mAs settings

Theoretically, higher mAs result in more photons to reach the detectors, result in less noise. From the reconstructed images, using higher mAs setting produced better image quality with less streaking artifacts. By increasing mAs, measured CT attenuation values were slightly increased (0.04% - 0.4%) within dark streak and decreased (0.26% - 0.31%) at bright streak region. Image noise was slightly reduced as mAs increased with reduction of 0.43% -1.58%. Statistical analysis showed that is no significant difference ( $P > 0.05$ ) in mean of CT attenuation and image noise.

For SNR value, it demonstrated that increased in mAs resulted in better SNR by slight increment of 3.3% in dark streak region and 0.3% increment in bright region. Figure 2 show the increment of SNR with increased mAs measured in bright streak region. From the results, it showed that a change in mAs does not really influence the CT attenuation, noise and SNR due to its slight changes.

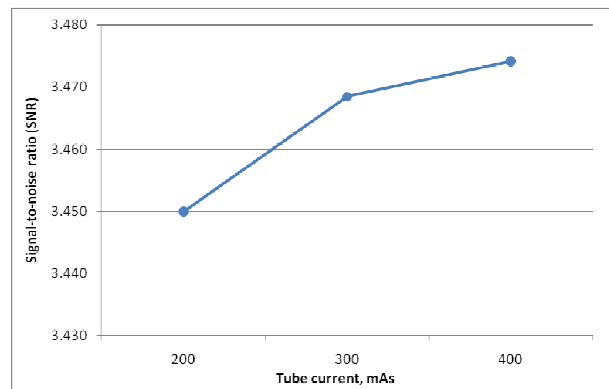


Fig. 3 The signal-to-noise ratio (SNR) for different tube current (mAs) setting within the bright streak region

#### C. Different reconstruction kernels

It can be observed that images reconstructed with sharp kernels (B70s and B80s) shows an improvement in spatial resolution, sharpness and edge detection with less streaking artifacts compared to images reconstructed with smooth kernels (B25s and B31s), as shown in Fig.4.

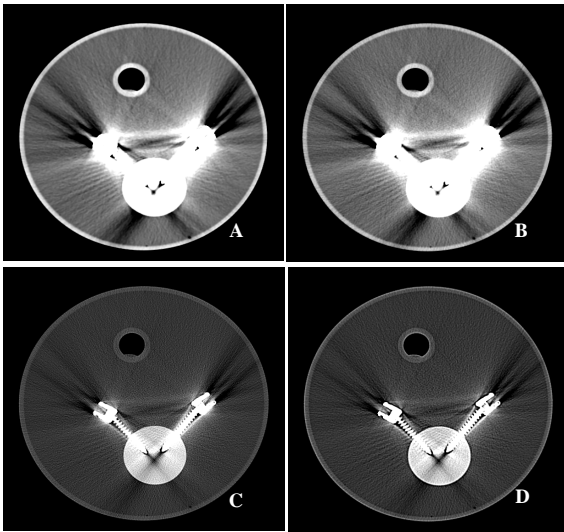


Fig. 4 The effect of 4 different convolution kernels; (A) B25s, (B) B31s, (C) B70s, and (D) B80s on metal streaking images. Images A and B are viewed using WL 40, WW 300 and images C and D are viewed using WL 450, WW 1500.

With wider window to view image C and D (Fig. 4), the shapes and edges of spinal screws were better defined and delineation of Teflon rod and screws were also improved using sharp kernel. The streak regions (dark and bright streaking) were also visually reduced by sharp kernel. However, the reduction of bright streaking region was more prominent than the dark streak using the bone kernel.

From the statistical analysis, it showed that reconstruction kernels had no significant influence on the measured CT attenuation ( $P > 0.05$ ), with small difference of 2.35 HU in the mean CT. The image noise measured in sharper kernel images was higher in streaking region (range = 108.0-184.0) as compared to smooth kernel (mean = 71.0 - 148.4).

This finding indicated that sharper kernel significantly increased the images noise with wider CT fluctuation. The mean different of noise between both kernels were statistically significantly ( $P < 0.05$ ) with increment of 54.78 in images of sharp kernel compared to images of smooth kernel. Correspondingly, our findings also similar with previous published data which stated that image reformatted with sharp kernel exhibit increased noise as compared to smooth kernel [2,12].

#### D. Different reconstruction thickness

The images reconstructed by different slice thickness shows different level of streaking severity. Thicker slice thickness produced less noisy image than thinner slice.

Measured CT attenuation values increased by 52% within dark streak but decreased at bright streak region by 53% as the slice thickness increased. Image noise is reduced in the thicker slice images by 53% reduction. The statistical results shows that difference in noise are statistically significantly ( $P < 0.001$ ) in bright streak but demonstrated no significant different in dark streak region ( $P > 0.05$ ).

For correlation analysis, result shows there is a significant ( $p$ -value = 0.001), positive high correlation ( $r = 0.993$ ) between the reconstruction thickness and the CT attenuation in the dark streak region but negative high correlation ( $r = -0.992$ ) for bright streak region.

The result shows significant correlation between the reconstruction thickness and the image noise ( $p$ -value = 0.002) with strong negative correlation ( $r = -0.985$ ). The negative correlation means that the noise decreased as the slice thickness increased.

From the results, it shows higher SNR as slice thickness become thicker by increment of 12.7%. Figure 4 show the increment of SNR as the slice thickness become thicker in bright streak region. Correlation analysis shows a significant strong correlation of SNR with the reconstruction thickness ( $p$ -value = 0.017 and  $r = 0.941$ ).

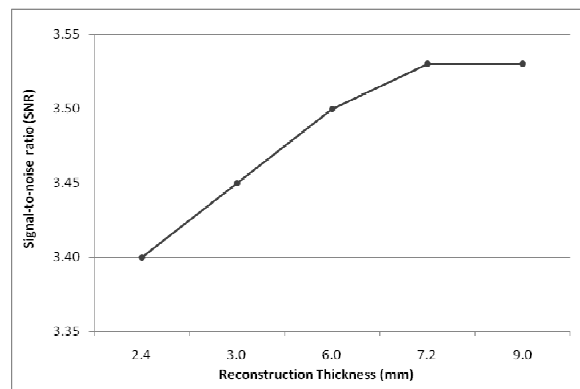


Fig. 4 The signal-to-noise ratio (SNR) for different reconstruction thickness within the bright streak region

#### IV. CONCLUSION

The scanning parameters should be chosen appropriately to achieve the acceptable image quality with the best diagnostic value. In the same time, we should avoid excessive radiation dose to patients throughout the examination.

The image reconstruction techniques also play a major role in reduction of streaking artifacts. A good reconstruction technique with modification in windowing offers great solution for artifact reduction.

#### ACKNOWLEDGEMENT

We thank the people from Dept. of Radiology, Hospital Universiti Sains Malaysia (HUSM), Kelantan, Malaysia for their help throughout the experiments. We also thanked Prototype and Development Centre (PDC), Malaysian Nuclear Agency, Malaysia for the fabrication of the Plexiglas phantom. Finally, we express our gratitude to OSA Technology Sdn. Bhd., Bangi, Selangor, Malaysia for providing metal rod samples and Dr. Abdul Halim, the Head of Orthopaedic Dept., HUSM, Kelantan, Malaysia for the spinal screw samples.

#### REFERENCES

- [1] E.E. Rutherford, L.J. Tarplett, E.M. Davies, J.M. Harley, L.J. King, "Lumbar spine fusion and stabilization: Hardware, techniques, and

- imaging appearances," *Radiographics*. Vol. 27 (6), pp. 1737 – 1749, 2007.
- [2] A.C. Douglas-Akinwande, K.A. Buckwalter, J. Rydberg, J.L. Rankin, R.H. Choplin, "Multichannel CT: Evaluating the spine in postoperative patients with orthopedic hardware," *Radiographics*. Vol. 26, pp. S97 – S110, 2006.
- [3] V.W. Lin, C.M. Bono, D.D. Cardenas, et. al, "Spinal cord medicine: principles and practice," 2nd ed., New York: Demos Medical Publishing, 2010, ch.3, pp. 34-45.
- [4] D.D.Robertson, P.J.Weiss, E.K. Fishman, D.Magid, and P.S. Walker, "Evaluation of CT techniques for reducing artifacts in the presence of metallic orthopedic implants," *J. of Comput. Assist. Tomogr.*, Vol.12, p.236-241, 1988.
- [5] J.F. Barret and N. Keat, "Artifacts in CT: Recognition and Avoidance," *RadioGraphics*, vol. 24, pp. 1679–1691, 2004.
- [6] M. Yazdi and L. Beaulieu, "Artifacts in spiral x-ray CT scanners: Problems and Solutions," *World Acad of Sci and Tech*, vol. 35, p.96-100, 2007.
- [7] M.J. Lee, S. Kim, S.A. Lee, H.T. Song, Y.M. Huh, D.H. Kim, S.H. Han, and J.S. Suh, "Overcoming Artifacts from Metallic Orthopedic Implants at High-Field-Strength MR Imaging and Multidetector CT," *RadioGraphics*, vol. 27, pp. 791–803, 2007.
- [8] P. Stradiotti, A. Curti, G. Castellazzi, and A. Zerbi, "Metal-related artifacts in instrumented spine. Techniques for reducing artifacts in CT and MRI: state of the art," *Eur Spine J*, vol.18, p.S102–S108, 2009.
- [9] M.L. Kataoka, M.G. Hochman, E.K. Rodriguez, P.P.Lin, S. Kubo, and V.D. Raptopoulos, "A Review of Factors That Affect Artifact From Metallic Hardware on Multi-Row Detector Computed Tomography," *Curr Probl Diagn Radiol*, vol.39, pp.125-136, 2010.
- [10] W. A. Kalender, "Computed Tomography: Fundamentals, System Technology, Image Quality, Applications," Munich, Germany: Publicis MCD, Verlag, 2000.
- [11] J. Paul, B. Krauss, R. Banckwitz, W. Maentele, R.W. Bauer, T.J. Vogl, "Relationship of clinical protocols and reconstruction kernels with image quality and radiation dose in a 128-slice CT scanner: Study with an antropomorphic and water phantom," *Eur. J. of Radiology*, in press (*doi:10.1016/j.ejrad.2011.01.078*),
- [12] I. Kassim, H. Joosten, J.C. Barnhoorn, B.J.M. Heijmen, and M.L.P. Dirkx, "Implications of artefacts reduction in the planning CT originating from implanted fiducial markers," *Med.Dosimetry*, in press (*doi: 10.1016/j.meddos.2010.02.002*).

**Noor Diyana Osman** is a PhD candidate in the Faculty of Health Science, Universiti Teknologi MARA, 42300 Puncak Alam, Malaysia. She is a fellow at Advanced Medical and Dental Institute (AMDI), Universiti Sains Malaysia, Malaysia (phone:603-32584300,email:diyanaosman.dina@gmail.com). This work is based in part on the PhD thesis of the author in partial fulfillment, of the PhD degree requirements.

**Prof Dr. Md Saion Salikin (PhD)** is the Deputy Dean (Research & Industrial Linkage) and senior lecturer in Faculty of Health Science, Universiti Teknologi MARA, 42300 Puncak Alam, Malaysia (phone: 6-03-32584304; e-mail: saion@salam.uitm.edu.my). His current research interest is in medical radiation physics, medical imaging, and dosimetry.

**Assoc. Prof Dr. M.Iqbal Saripan (PhD)** is a senior lecturer in Department of Computer and Communication Systems Engineering, Faculty of Engineering, Universiti Putra Malaysia, 43400 Serdang, Selangor, Malaysia. (e-mail: iqbal@eng.upm.edu.my). His current research interest is in digital image/signal processing, medical imaging, and biomedical engineering. The author is a member of Institute of Electrical and Electronics Engineers (MIEEE), International Association of Engineers (Member IAENG), and Graduate Member, Board of Engineers Malaysia (GradBEM).